Progress In Electromagnetics Research, Vol. 128, 313–329, 2012

PRINTED WIDEBAND ANTENNA WITH CHIP-CAPACITOR-LOADED INDUCTIVE STRIP FOR LTE/GSM/UMTS WWAN WIRELESS USB DONGLE APPLICATIONS

Y.-L. Ban[1, *], J.-H. Chen[1], S.-C. Sun[1], J. L.-W. Li[1], and J.-H. Guo[2]

[1]Institute of Electromagnetics, University of Electronic Science and Technology of China, Chengdu 611731, China

[2]Department of Biomedical Engineering, Nanyang Technological University, 70 Nanyang Drive, Singapore 63745, Singapore

Abstract—This paper proposes a planar printed wideband antenna for eight-band LTE/GSM/UMTS WWAN wireless USB dongle applications. An inductive shorted strip with a chip capacitor loaded is employed in order to improve the characteristics of small-size terminal antennas which usually have a narrow band over the LTE700/GSM850/900 (698–960 MHz) operation. While the desired upper band is mainly realized by the rectangular radiating patch, covering DCS1800/PCS1900/UMTS2100/LTE2300/2500 (1710–2690 MHz) band. Easily printed on a 0.8-mm thick FR4 dielectric substrate of size $20 \times 70\,\text{mm}^2$, the proposed antenna structure occupies a compact size of $20 \times 19\,\text{mm}^2$. Then the proposed design can be attached to laptop computer by the USB interface. Good radiation efficiency and antenna gain for frequencies over the desired operating bands is obtained. Detailed design considerations of the proposed antenna are described, and both experimental and simulation results are also presented and discussed.

1. INTRODUCTION

Recently, wireless universal serial bus (USB) dongles with plug-and-play functionality have attracted more and more wideworld attention of researchers, especially for the 3G and 4G mobile communication systems which should be capable of accommodating

Received 28 February 2012, Accepted 17 May 2012, Scheduled 1 June 2012

* Corresponding author: Yong-Ling Ban (byl@uestc.edu.cn).

higher communication data rate than current systems. By a wireless USB dongle device attached to laptops, one can receive and transmit wireless data anytime and anywhere. However, it has been a continuous challenge in the design of wideband or multiband internal mobile antennas with the attractive features of compact size, simple structure, low profile, and ease of fabrication [1–8]. In this case, a number of suitable antenna designs with different geometries for wireless USB dongle have also been experimentally characterized [9–14]. The designed antennas occupying a small size of about $20 \times 10 \times 5\,\text{mm}^3$ on the system circuit board and are easy to fabricate at low-cost as the reported wideband wireless USB dongle antennas in Refs. [9, 10], which can cover partial operating bands of the WiBro (2300–2390 MHz), Bluetooth (2400–2484 MHz), WLAN (2400–2485 and 5150–5850 MHz), WiMAX (2500–2690/3300–3800/5250–5850 MHz) and S-DMB (2605–2655 MHz) operation. In addition, the antennas [11–13] can generate multiple resonances covering UWB frequency band of 3.1–10.6 GHz. A novel planar printed ultra-wideband antenna with distributed inductance for wireless USB dongle attached to laptop computer, has been demonstrated, which covers the whole LTE/GSM/UMTS WWAN in the 698–960 and 1710–2690 MHz frequency band in Ref. [14]. However, the studies and designs of the ultra-wideband LTE/GSM/UMTS WWAN antennas are not enough.

Moreover, due to the recent introduction of the long term evolution (LTE) operation for mobile broadband services, the mobile devices such as laptop computers and mobile phones in the near future are expected to be capable of both the LTE and wireless wide area network (WWAN) operations. For this application, the internal antenna in the mobile devices should provide two wide operating bands of at least 698–960 and 1710–2690 MHz to cover three LTE bands (LTE700/2300/2500 in the 698–787/2300–2400/2500–2690 MHz bands) and five usual bands (GSM850/900/DCS1800/PCS1900/UMTS2100 in the 824–894/880–960/1710–1880/1850–1990/1920–2170 MHz bands). Based on the current of wideband mobile antennas, the wireless USB dongle antennas [9–13] can not cover overall LTE/GSM/UMTS operation. To achieve wider operating bandwidth, several techniques are developed and studied, one of which is the approach of the lumped element loading [2, 5, 15–17]. In Ref. [15], a small-size annular slot antenna with miniaturized slot shrunk by a loaded capacitor has been realized. A chip inductor is loaded in the printed monopole antennas in [2] and [5] to decrease resonant length of the fundamental mode and improve impedance matching over the desired operating bands. Several planar small-size wideband internal mobile phone antenna structures

formed by a radiating strip with a chip-capacitor-loaded for achieving LTE/GSM/UMTS multiband operation are proposed in Refs. [16, 17]. Up to now, few wireless USB dongle antennas, which cover whole LTE/GSM/UMTS operation [14], have been reported in the open literature.

For this purpose, based on the reported designs [18–24], we propose a planar printed wideband antenna that not only occuyies compact structure size printed on the system circuit board but also provides a whole eight-band LTE/GSM/UMTS operation in this article. The presented design shows a simpler structure, comprising of a rectangular radiating patch with a chip-capacitor-loaded shorted inductive strip and a matching capacitor, than the reported wideband wireless USB dongle antennas [9–13]. Further, the proposed antenna is a planar structure and is suitable to be disposed on a small no-ground board space of $20 \times 19\,\text{mm}^2$, which makes the antenna promising to be applied in the modern slim wireless USB dongles. Detailed operating principle of the presented antenna is described in the following section. The antenna is also fabricated and tested, and the obtained results are presented and studied. Having a low profile and printed structure, good radiation characteristics, as well as wide operating bandwidth, the proposed antenna can be considered a good solution for future wireless USB dongle applications.

2. PROPOSED ANTENNA CONFIGURATION

Figure 1 shows the configuration of the proposed, planar printed patch antenna with a chip-capacitor-loaded ($C1 = 6\,\text{pF}$) inductive strip and a matching chip capacitor ($C2 = 1.5\,\text{pF}$) and printed on the top of the 0.8-mm thick FR4 substrate (size $20 \times 70\,\text{mm}^2$, relative permittivity is 4.4 and loss tangent is 0.025). The presented design is placed on a clearance area of size $20 \times 19\,\text{mm}^2$, where no grounding layout occupies on the back side of the system circuit board. A 50-Ω microstrip feed line is employed to excite the proposed antenna at the feeding point A, and the long inductive strip is shorted to the system ground plane of the wireless USB dongle at the shorting point B. Hence, there is a separation distance of 0.5 mm between the radiating patch and the system ground plane of the wireless USB dongle to obtain better impedance matching of the antenna. In this study, the USB dongle can be connected to laptops through the USB interface, and the laptop has a 90° angle between the laptop's keyboard and display (both size is $200 \times 300\,\text{mm}^2$ [14]) in order to simulate the practical issue.

The proposed antenna mainly comprises two portions: a radiating patch and a long inductive strip with a chip capacitor embedded. For

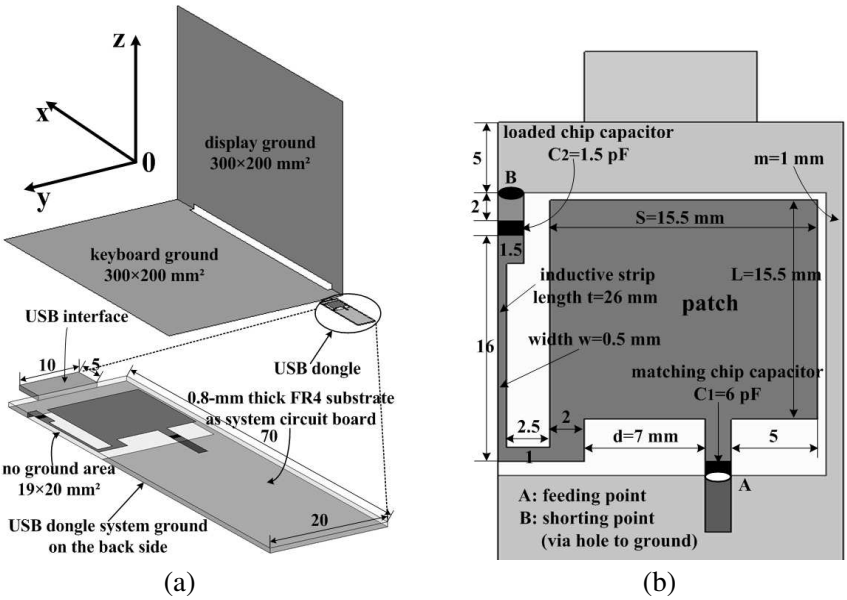

Figure 1. Proposed antenna configuration: (a) Geometry of the wideband antenna for wireless USB dongle application. (b) Detailed dimensions of the antenna (units: mm).

the desired upper band of DCS1800/PCS1900/UMTS2100/LTE2300 /2500 (1710–2690 MHz) operation, the rectangular radiating patch can generate two resonant modes at about 1800 MHz and 2800 MHz with the help of the long inductive strip. While the dual-resonance excitation for the antenna's lower band of LTE700/GSM850/900 (698–960 MHz) operation can be obtained. There are two reasons. Firstly, the long inductive strip provides a fundamental resonant path at around 800 MHz, and the input resistance level which is usually much larger than 50 Ω at around the two resonances can be significantly decreased. Secondly, the loaded chip capacitor can contribute additional capacitance to compensate for the large input inductance seen in the antenna's lower band at around 550 MHz. This can lead to an additional close to zero reactance occurred in the proximity of the existing zero reactance, that is, there can be two zero reactance or two resonances occurred in the desired 698–960 MHz band. These two conditions result in a dual-resonance excitation with good impedance matching for the antenna's lower band. Hence, a wide lower band to cover the desired WWAN operation in the LTE700/GSM850/900 band can be achieved for the antenna design.

Also note that the two chip capacitors can be properly adjusted to enhance the antenna's input impedance to achieve the desired eight-band operating bands.

The final dimensions for the prototype are attained by the parametric studies with the aid of the electromagnetic-field simulation tool, Ansoft HFSS. To clearly illustrate the process of the antenna design and provide antenna engineers with useful information about the design and optimization of the proposed antenna, detailed parametric study is given in the following section. The key parameter effects in return loss are theoretically studied. Each investigation is performed with only one varying parameter while others keep the same as the mentioned in Figure 1. Firstly, L, the length of the rectangular radiating patch, is a key factor to form the desired upper band and first studied in Figure 2(a). With the increase of the length L, the impedance matching of the DCS1800/PCS1900/UMTS2100 band is improved effectively, and the results show that the desired lower band of 698–960 MHz is affected hardly. Similar behavior can be seen in Figure 2(b), where the simulated return loss is presented by varying the width S of the rectangular radiating patch. It is seen that when S is varied from 10.5 to 15.5 mm, the second two resonant modes at about 1800 MHz and 2800 MHz will shift down to cover 1710–2690 MHz.

To analyze the several excited resonant modes, Figure 3 plots the effects of the embedded matching chip capacitor on the proposed antenna. In Figure 3(a), simulated results for the value $C1$ varied from 2.2 to 7.6 pF reveal that different chip capacitors have significant influences on the desired lower input impedance. For $C1$ is 2.2 pF, poor impedance matching over the antenna's lower band is seen (there is only one resonant mode generated at around 900 MHz, thus this leads to the achieved lower bandwidth can not cover the

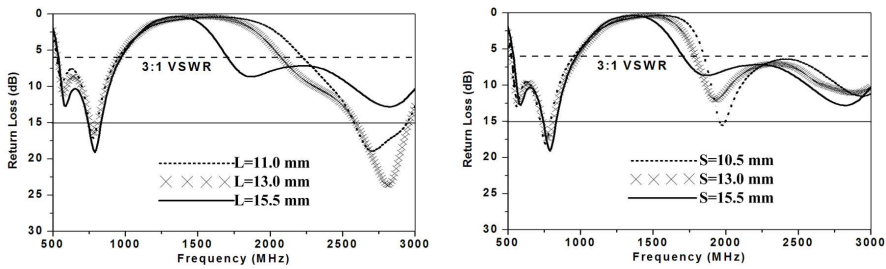

Figure 2. Simulated return loss as a function of (a) the length L and (b) the width of the rectangular radiating patch S.

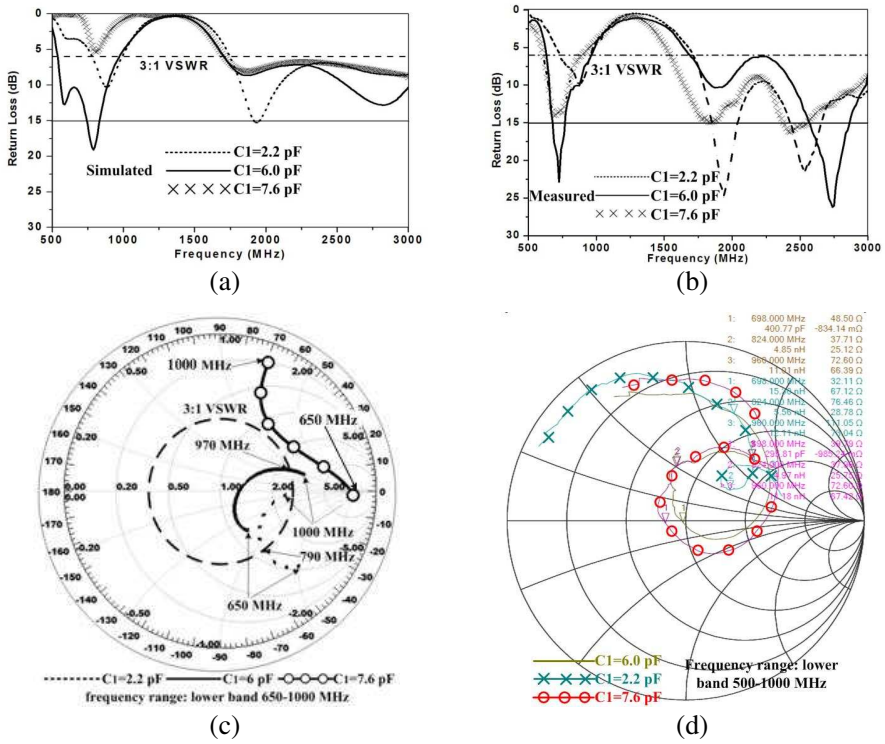

Figure 3. (a) Simulated and (b) measured return loss for different values $C1$ of the matching chip capacitor. (c) Simulated and (d) measured impedance matching on Smith chart for different values $C1$ of the matching chip capacitor.

LTE700/GSM850/900 operation), and the upper bandwidth is also not enough. In addition, the lower band can not be realized completely, but the upper operating band is perfect if the matching chip capacitor is chosen as 7.6 pF. While the capacitor $C1$ equals to 6 pF further, improved impedance matching for the desired lower resonant modes at about 550 MHz and 800 MHz are not only obtained, but also the upper resonant modes can cover GSM1800/1900/UMTS2100/LTE2300/2500 in operation. Similar results can be seen in Figure 3(b), where measured return loss curves are given. Then, the corresponding input impedance results of the lower band on the Smith chart are shown in Figures 3(c) and (d). Results indicate that the chip capacitor has strong effects on the impedance matching over the lower band. It is clearly seen that, compared to the other chip capacitors, the impedance

matching over the desired lower band of the 698–960 MHz for the proposed design ($C1 = 6$ pF) is better. There are some disagreements between the measured and simulated of return loss and Smith chart; this is mainly because of errors of fabrication (properties of used FR4 substrate, size errors of fabrication) and testing (effects of coaxial cable introduced for testing).

Effects of the location d of the feeding strip are studied in Figure 4(a). Results of the simulated return loss for d varied from 3.5 to 10.5 mm show that the different locations greatly affect the impedance matching on the whole upper bandwidth coverage. Especially for $d = 10.5$ mm, there is only one resonance at about 2500 MHz, the lower bandwidth will be wider although. The simulated return loss curves with different width m are plotted in Figure 4(b). When the m is decreased from 1.5 to 0.3 mm, the antenna's input impedance is improved greatly. However, in the design it is chosen as 1.0 mm after considering that high-speed USB data signal lines will be arranged on the signal ground and the signal ground with too small width can not shield off the high-speed USB data signal for practical USB dongle applications. From the parametric study above, the preferred location d and width m are chosen to be 7 mm and 1 mm, respectively, in the final antenna dimensions.

Figure 5(a) displays the effects of the length P of the wireless USB dongle system ground plane on the simulated return loss. It is clearly seen that the desired lower bandwidth is strongly controlled by the length P. These results confirm that the successful lower bandwidth of 698–960 MHz coverage needs the help of the USB dongle system ground plane and laptop system ground plane. And, there is no resonant mode generated over the desired lower band shown in Figure 5(b). That is, the proposed design is an entire structure formed by the radiating patch

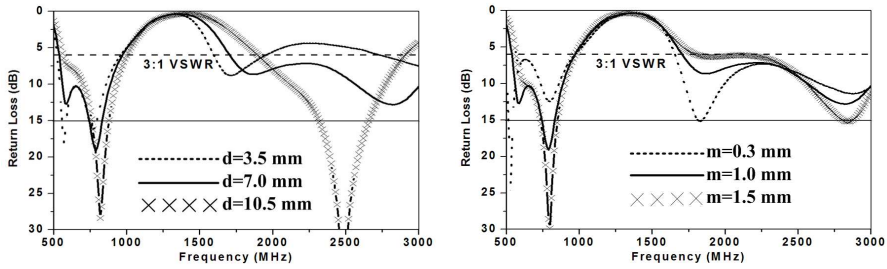

Figure 4. Simulated return loss as a function of (a) the location d of the feeding strip and (b) the width m of the high-speed data lines.

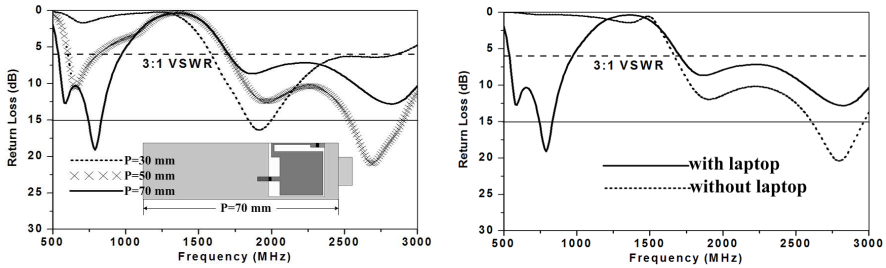

Figure 5. Simulated return loss as a function of (a) the length P of the wireless USB dongle system ground plane and (b) the cases with or without the laptop.

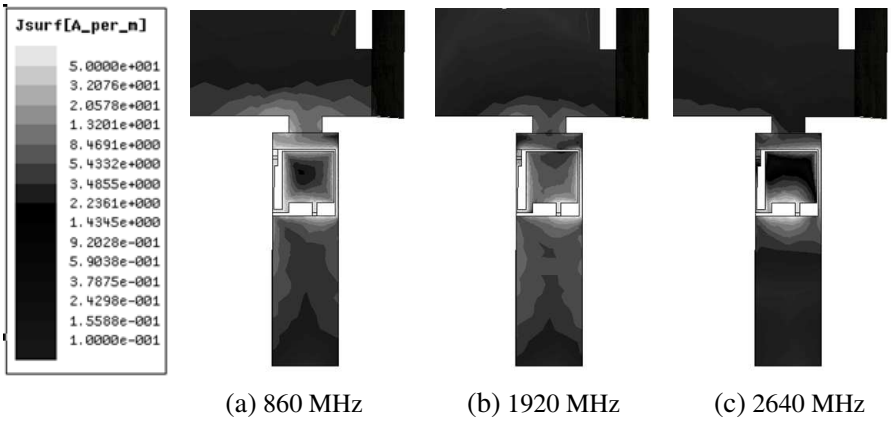

Figure 6. Simulated surface current distributions at (a) 860 MHz, (b) 1920 MHz and (c) 2640 MHz for the proposed antenna.

with a chip-capacitor-loaded inductive strip, the USB dongle system ground plane and laptop system ground plane, and the whole antenna configuration fabricates an effective radiating system.

In addition, the simulated current distributions of the proposed antenna at 860 MHz, 1920 MHz and 2640 MHz are presented in Figures 6(a)–(c), respectively. It is first seen from Figure 6(a) for 860 MHz that the excited surface currents flow around the inductive strip to the USB dongle system ground plane and laptop system ground plane, which means that the lower resonant modes are mainly contributed by the inductive strip, the USB dongle system ground plane and laptop system ground plane. Besides, the surface currents of

the upper frequencies at 1920 MHz and 2640 MHz seen in Figures 6(b) and (c) are different from those shown in Figure 6(a). For the desired upper band, the strong current distributions are observed on the rectangular radiating patch and the partial ground plane (close to the patch) of the USB dongle ground plane. Especially for 2640 MHz shown in Figure 6(c), there are only strong currents around the patch that is close to the feeding strip and indicates the patch has a significant effect on the successful excitation of the upper resonant modes. These results indicate that USB dongle system ground plane and laptop system ground plane are also important radiating parts at 860 MHz, 1920 MHz and 2640 MHz.

3. BANDWIDTH ENHANCEMENT BY THE INDUCTIVE STRIP WITH CAPACITOR LOADED

In this section, after studying the common parameters of the proposed antenna, we investigate the significant parameters, which are very helpful for the bandwidth enhancement of the whole desired operating band, especially for LTE700/GSM850/900 operation. Figure 7(a) shows the results of the simulated return loss for the proposed antenna, the corresponding antenna without chip-capacitor-loaded (Ref 1) and the corresponding antenna without inductive strip (Ref 2). The corresponding dimensions of the three cases are all the same as given in Figure 1. Results clearly indicate that the proposed antenna's lower band is mainly contributed from the chip-capacitor-loaded, and there is only one resonant mode excited at around 1500 MHz for Ref 2.

The above results can be well illustrated with the help of Figures 7(b) and (c), where show the simulated input impedance versus frequency for the proposed antenna, Ref 1 and Ref 2. For the lower band shown in Figure 7(b), mainly owing to the contributed capacitance of the chip-capacitor-loaded, the input reactance (Im curve) of the proposed antenna is greatly decreased as compared to that of the Ref 1. This behavior leads to more zero or close to zero reactance occurred for the proposed antenna, thus there are two resonant modes at about 550 MHz and 800 MHz, resulting in the dual-resonance excitation seen for the antenna's lower band in Figure 7(a).

In addition, Figure 7(c) shows the real part (Re) and imaginary part (Im) of the simulated input impedance of the proposed and the Ref scheme 2. It is clearly seen that owing to the use of the long strip in the proposed antenna, the high-impedance level of the resonant mode at the desired operating band is effectively decreased and forms four null points in imaginary part when compared with that for the reference antenna 2, then this leads to the excitation of two resonant

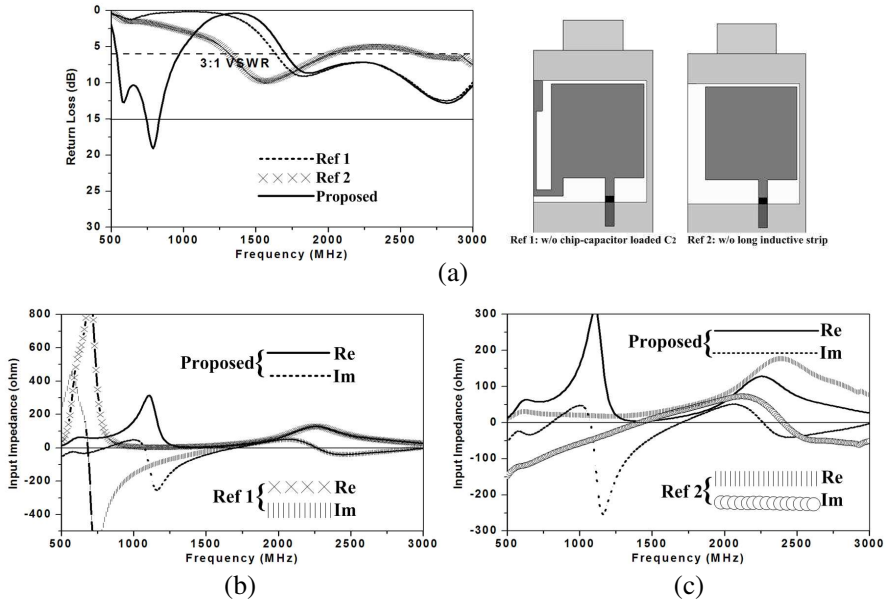

Figure 7. (a) Simulated return loss for the proposed antenna, the corresponding antenna without chip-capacitor-loaded (Ref 1) and the corresponding antenna without inductive strip (Ref 2), (b) comparison of the simulated input impedance for the proposed antenna and Ref 1 and (c) comparison of the simulated input impedance for the proposed antenna and Ref 2.

modes at the desired upper band around 1800 MHz and 2800 MHz. From the above analysis, it can be good illustrated that the long strip acts as a distributed inductance's presence and can improve impedance matching over the desired lower operating band, generating multiple resonances to cover LTE700/GSM850/900 operation.

It can be seen from Figure 8 that varying the chip-capacitor-loaded $C2$ will affect the desired lower bandwidth coverage. Figures 8(a) and (b) show return loss as a function of the capacitance $C2$ of the chip-capacitor-loaded in the inductive strip. The increasing capacitance ($C2 = 3.9$ pF in the study) causes that both the second and third resonant modes shift up, resulting in that the proposed antenna can not cover 698–960 MHz and DCS1800 (1710–2690 MHz) operation effectively in this case. If $C2$ is chosen to be 3.9 pF, the upper impedance bandwidth is increased. However, there is no the desired lower bandwidth achieved. Only the capacitance of the chip-capacitor-loaded equals to 1.5 pF, the desired bandwidth is met. To illustrate

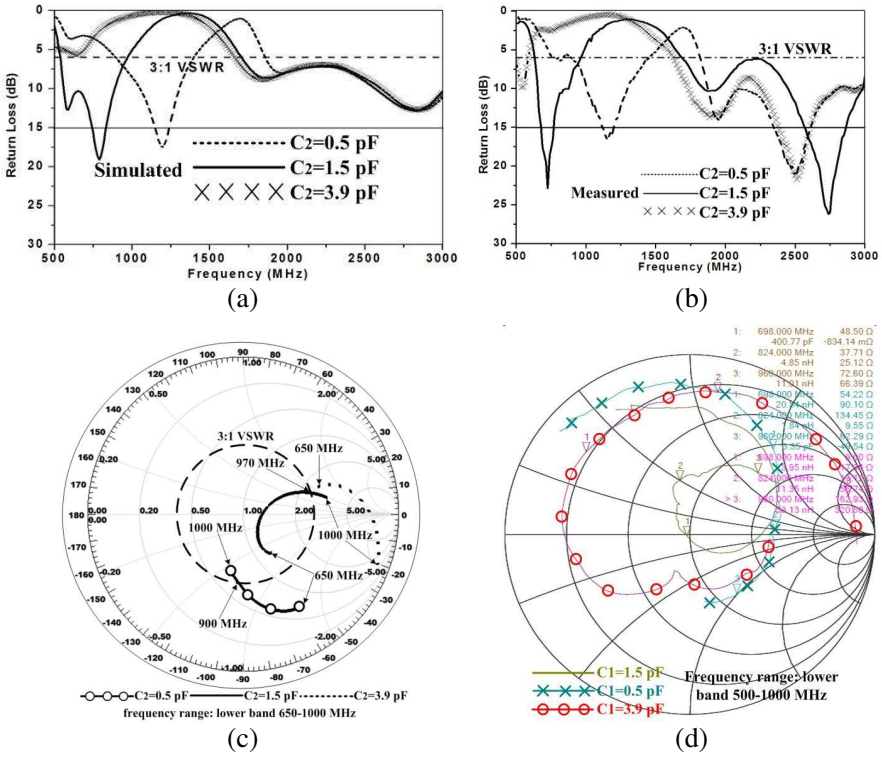

Figure 8. (a) Simulated and (b) measured return loss for different values $C2$ of the chip-capacitor-loaded. (c) Simulated and (d) measured impedance matching on Smith chart for different values $C2$ of the chip-capacitor-loaded.

the presence of the chip-capacitor-loaded in depth, the simulated and measured input impedance curves on the Smith chart versus frequency for the proposed antenna are plotted in Figures 8(c) and (d). In the Figure 8(c), only the impedance curves for the frequency range of 650–1000 MHz (the presented antenna's lower band) are given. It is found that, compared to the capacitance 0.5 or 3.9 pF, the loop of the impedance curve for the proposed design ($C2 = 1.5$ pF) from 698 to 960 MHz is more close to 50 ohm matching point in the circles, which can cover LTE700/GSM850/900 operation with 3 : 1 VSWR.

Also, a study on the parameter t in length and w in width of the inductive strip is conducted in Figure 9. Results for the length t varied from 22 to 28 mm are presented in Figure 9(a); other dimensions of the proposed antenna are the same as given in Figure 1. Results display

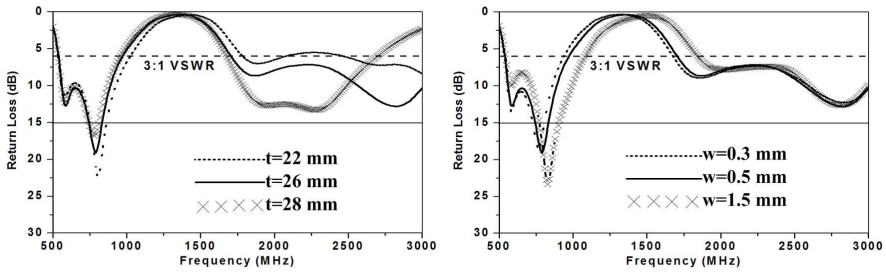

Figure 9. Simulated return loss as a function of (a) the length t and (b) the width w of the inductive strip.

that the second resonant frequency is lowered and the impedance matching of the third and fourth resonant modes are improved, when the length t is increased from 22 to 28 mm. Thus, the desired GSM900 band and LTE2500 band can not be achieved. If t equals to 22 mm, the impedance matching of the upper band will be poor. Besides, Figure 9(b) shows the simulated return loss as a function of the width w. When w equals to 0.3 or 1.5 mm, the desired lower and upper bandwidth is not enough from the results. Considering the overall performance of the different values of the width in the study, w is selected to be 0.5 mm finally.

4. MEASURED RESULTS AND DISCUSSION

To verify our design, an antenna prototype with optimized dimensions is fabricated as shown in Figure 10(a). The return loss is measured by an Agilent vector network analyzer N5247A. The measured and simulated return loss curves of the proposed antenna are given in Figure 11, where about 330 MHz from 635 MHz to 965 MHz and 1310 MHz from 1690 MHz to 3000 MHz with VSWR $<$ 3 bandwidth of the desired lower LTE700/GSM850/900 band and upper DCS1800/PCS1900/UMTS2100/LTE2300/2500 band is observed respectively. Notice that the 3 : 1 VSWR bandwidth definition is widely used in the internal mobile device antenna for WWAN operation [3–5, 14, 17]. Obviously, the measured return loss reasonably agrees with the simulated one, with an acceptable frequency discrepancy, which may be caused by the substrate property and the introduced coaxial cable in the experiment.

The radiation patterns of the proposed antenna are measured in microwave chamber SATIMO shown in Figure 10(b). To obtain

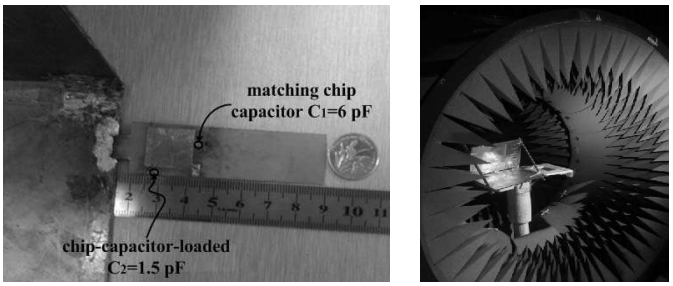

(a) (b)

Figure 10. Photo of (a) the manufactured printed antenna for wireless USB dongle applications and (b) the proposed antenna measured in microwave chamber SATIMO.

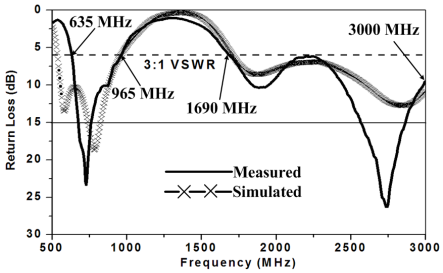

Figure 11. Simulated and measured return loss of the proposed antenna.

the performance of the proposed antenna overall, the measured and simulated far-field radiation patterns at 860 MHz, 1920 MHz and 2640 MHz are plotted in Figure 12. At 860 MHz in Figure 12(a), smooth variations in the vertical polarization $E\theta$ over all of the φ angles are seen in the azimuthal plane (x-y plane), which can provide good coverage for LTE700/GSM850/900 operation. According to these curves at the frequencies of 1920 MHz and 2640 MHz shown in Figures 12(b) and (c) respectively, it can be seen that more variations in radiation patterns compared with those in Figure 12(a) are observed. This is in part owing to the nulls of the excited surface currents on the system ground plane at higher frequencies. However, there are a few differences between measured and simulated patterns at 860 MHz, 1920 MHz and 2640 MHz, and the measured results of the proposed antenna are less than the simulated results. In fact, this is owing to that the practical coaxial cable introduced leads to variations of the whole radiation structure and power loss in the experiment, whereas the cable is no existence in the simulation.

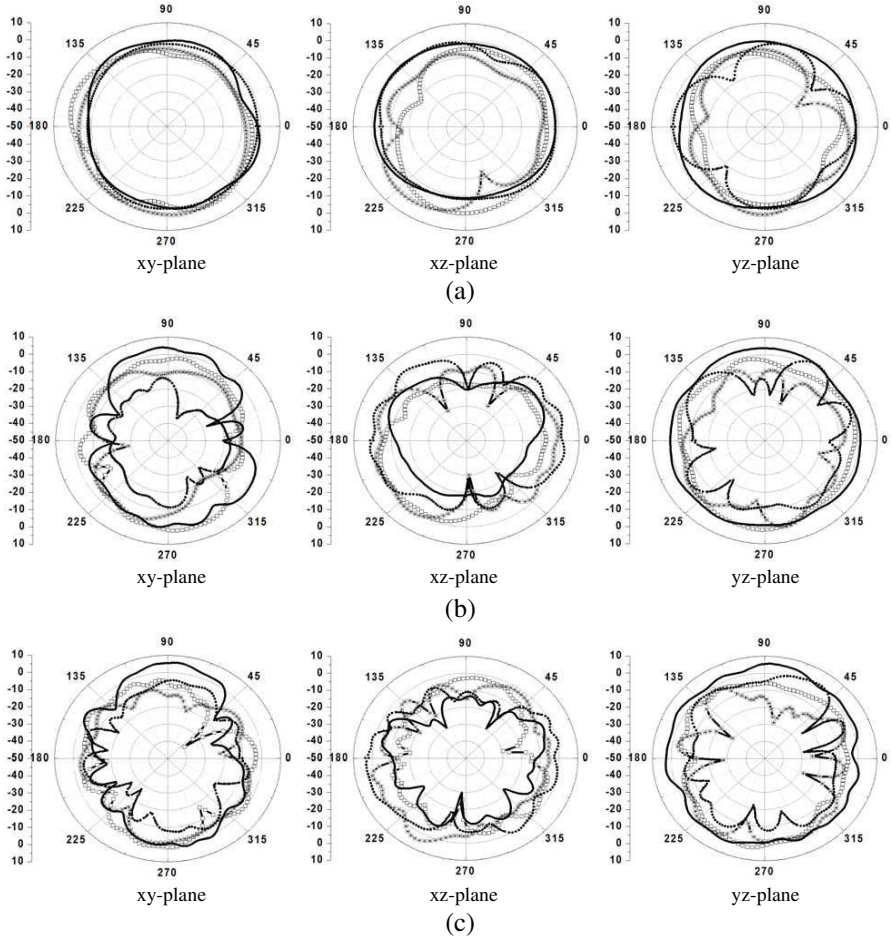

Figure 12. Measured and simulated 2-D radiation patterns at (a) 860 MHz, (b) 1920 MHz and (c) 2640 MHz for the proposed antenna ($\square\square\square$ E_φ (measured), $***$ E_θ (measured), — E_φ (simulated), $\cdots$ E_θ (simulated)).

Measured and simulated peak antenna gain and measured radiation efficiency curves of the proposed antenna are displayed in Figure 13. For the lower bandwidth of LTE700/GSM850/900 in Figure 13(a), the simulated peak antenna gain ranges from 2.1 to 3.9 dBi, while the corresponding measured maximum peak antenna gains across the operating band are close to 3.2 dBi with the gain variations of 1.5 dBi and the measured radiation efficiency is from 51% to 78%. For the upper band shown in Figure 13(b), the measured peak

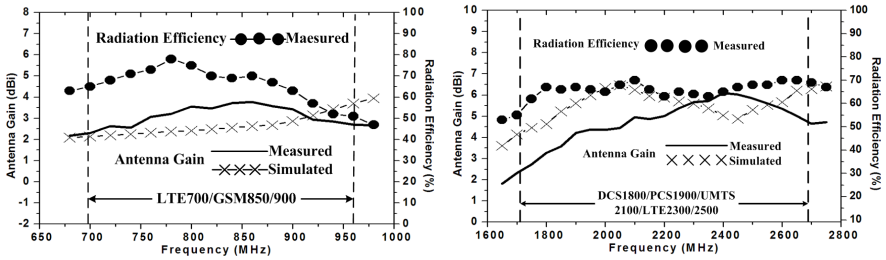

Figure 13. Measured and simulated peak antenna gain and simulated radiation efficiency across the operating band for the proposed antenna: (a) The lower operating bands LTE700/GSM850/900. (b) The upper operating bands DCS1800/PCS1900/UMTS2100/ LTE2300/2500.

antenna gain for DCS1800/PCS1900/ UMTS2100/LTE2300/2500 operation varies from about 2.5 to 6.1 dBi and the simulated peak antenna gain for the upper band is 4.1–6.4 dBi, while the measured radiation efficiency ranges is about 65%. Obviously, the above results of the obtained radiation characteristics indicate that the presented antenna is a good solution for practical wireless USB dongle attached to laptop applications.

5. CONCLUSION

A planar printed wideband antenna has been presented for wireless USB dongle applications. Consisting of the radiating patch with a chip-capacitor-loaded inductive strip and a chip matching capacitor, the achieved impedance bandwidth for VSWR < 3 of the proposed antenna has covered the desired lower band of 698–960 MHz and desired upper band of 1710–2690 MHz well. Detailed parametric study has provided antenna engineers with useful information about the design and optimization of the proposed antenna. The main advantage of this scheme is that the presented antenna has a simple structure and wide LTE/WWAN operation. With acceptable radiation patterns across the operating bandwidth and an average efficiency of 70%, the design is attractive for use in wireless USB dongle applications.

REFERENCES

1. Sze, J.-Y. and Y.-F. Wu, "A compact planar hexa-band internal antenna for mobile phone," *Progress In Electromagnetics Research*, Vol. 107, 413–425, 2010.

2. Luo, Q., J. R. Pereira, and H. M. Salgado, "Compact printed monopole antenna with chip inductor for WLAN," *IEEE Antennas Wireless Propag. Lett.*, Vol. 10, 880–883, 2011.
3. Kusuma, A. H., A.-F. Sheta, I. Elshafiey, Z. Siddiqui, M. A. Alkanhal, S. Aldosari, and S. A. Alshebeili, "A new low SAR antenna structure for wireless handset applications," *Progress In Electromagnetics Research*, Vol. 112, 23–40, 2011.
4. Chen, J. H., Y. L. Ban, H. M. Yuan, and Y. J. Wu, "Printed coupled-fed PIFA for seven-band GSM/UMTS/LTE WWAN mobile phone," *Journal of Electromagnetic Waves and Applications*, Vol. 26, Nos. 2–3, 390–401, 2012.
5. Wong, K. L. and C. T. Lee, "Small-size wideband monopole antenna closely coupled with a chip-inductor-loaded shorted strip for 11-band WWAN/WLAN/WiMAX operation in the slim mobile phone," *Microw. Opt. Technol. Lett.*, Vol. 53, No. 2, 361–366, Feb. 2011.
6. Tiang, J. J., M. T. Islam, N. Misran, and J. S. Mandeep, "Slot loaded circular microstrip antenna with meandered slits," *Journal of Electromagnetic Waves and Applications*, Vol. 25, No. 13, 1851–1862, 2011.
7. Zhou, B., H. Li, X. Y. Zou, and T. J. Cui, "Broadband and high-gain planar vivaldi antennas based on inhomogeneous anisotropic zero-index metamaterials," *Progress In Electromagnetics Research*, Vol. 120, 235–247, 2011.
8. Cao, W. Q., B. N. Zhang, T. B. Yu, A. J. Liu, S. J. Zhao, D. S. Guo, and Z. D. Song, "Single-feed dual-band dual-mode and dual-polarized microstrip antenna based on metamaterial structure," *Journal of Electromagnetic Waves and Applications*, Vol. 25, No. 13, 1909–1919, 2011.
9. Viani, F., L. Lizzi, R. Azaro, and A. Massa, "A miniaturized UWB antenna for wireless dongle devices," *IEEE Antennas Wireless Propag. Lett.*, Vol. 7, 714–717, 2008.
10. Liu, W. C. and Y. L. Chen, "Compact strip-monopole antenna for WLAN-band USB dongle application," *Electronics Lett.*, Vol. 47, 479–480, 2011.
11. Su, S. W., J. H. Chou, and K. L. Wong, "Internal ultrawideband monopole antenna for wireless USB dongle application," *IEEE Trans. Antennas Propag.*, Vol. 55, 1180–1183, Apr. 2007.
12. Gong, J. G., Y. C. Jiao, Q. Li, Y. Song, and J. Wang, "Compact internal wideband antenna for wireless USB dongle application," *IEEE Antennas Wireless Propag. Lett.*, Vol. 9, 879–882, 2010.

13. Tu, S., Y. C. Jiao, Z. Zhang, Y. Song, and S. M. Ning, "Small internal 2.4-GHz/UWB antenna for wireless dongle applications," *IEEE Antennas Wireless Propag. Lett.*, Vol. 9, 284–287, 2010.
14. Ban, Y. L., H. M. Yuan, J. H. Chen, L. W. Li, and Y. J. Wu, "A novel ultra-wideband antenna with distributed inductance for wireless USB dongle attached to laptop computer," *Journal of Electromagnetic Waves and Applications*, Vol. 26, Nos. 2–3, 179–191, 2012.
15. Hong, C. S., "Small annular slot antenna with capacitor loading," *Electronics Letters*, Vol. 36, No. 2, 110–111, Jan. 2000.
16. Gokhan, M., S. Gupta, K. Sertel, and J. L. Volakis, "Small wideband double-loop antennas using lumped inductors and coupling capacitors," *IEEE Antennas Wireless Propag. Lett.*, Vol. 10, 107–110, 2011.
17. Wong, K. L. and Y. W. Chang, "Internal eight-band WWAN/LTE handset antenna using loop shorting strip and chip-capacitor-loaded feeding strip for bandwidth enhancement," *Microw. Opt. Technol. Lett.*, Vol. 53, No. 6, 1217–1222, Jun. 2011.
18. Liao, W.-J., S.-H. Chang, and L.-K. Li, "A compact planar multiband antenna for integrated mobile devices," *Progress In Electromagnetics Research*, Vol. 109, 1–16, 2010.
19. Chen, W. S. and B. Y. Lee, "A meander PDA antenna for GSM/DCS/PCS/UMTS/WLAN applications," *Progress In Electromagnetics Research Letters,* Vol. 14, 101–109, 2010.
20. Kasabegoudar, V. G., "Low profile suspended microstrip antennas for wideband applications," *Journal of Electromagnetic Waves and Applications*, Vol. 25, No. 13, 1795–1806, 2011.
21. Chiu, C.-W. and C.-H. Chang, "Multiband folded loop antenna for smart phones," *Progress In Electromagnetics Research*, Vol. 102, 213–226, 2010.
22. Elsharkawy, Z. F., A. A. Saharshar, S. M. Elhalafawy, and S. M. Elaraby, "Ultra-wideband A-shaped printed antenna with parasitic elements," *Journal of Electromagnetic Waves and Applications*, Vol. 24, Nos. 14–15, 1909–1919, 2010.
23. Lin, D. B., I. T. Tang, and M. Z. Hong, "A compact quad-band PIFA by tuning the defected ground structure for mobile phones," *Progress In Electromagnetics Research B*, Vol. 24, 173–189, 2010.
24. Nishamol, M. S., V. P. Sarin, D. Tony, C. K. Anandan, P. Mohanan, and K. Vasudevan, "A broadband microstrip antenna for IEEE 802.11a/WiMAX/HIPERLAN2 applications," *Progress In Electromagnetics Research*, Vol. 19, 155–161, 2010.